Available online at www.sciencedirect.com
SCIENCE DIRECT®
Journal of Solid State Chemistry 177 (2004) 3735–3742
JOURNAL OF SOLID STATE CHEMISTRY
www.elsevier.com/locate/jssc

Preparation of three terbium complexes with *p*-aminobenzoic acid and investigation of crystal structure influence on luminescence property

Chao-Hong Ye[a], Hao-Ling Sun[a], Xin-Yi Wang[a], Jun-Ran Li[a,*], Dao-Bo Nie[a], Wen-Fu Fu[b], Song Gao[a,*]

[a]*State Key Laboratory of Rare Earth Materials Chemistry and Applications, College of Chemistry and Molecular Engineering, Peking University, Haidian District, Number 202, Chengfu Road, Beijing 100871, China*
[b]*Technical Institute of Physics and Chemistry, Chinese Academy of Science, Beijing 100101, China*

Received 23 January 2004; received in revised form 13 June 2004; accepted 17 June 2004
Available online 27 August 2004

Abstract

Three new rare earth *p*-aminobenzoic acid complexes, $[Tb_2L_6(H_2O)_2]_n$ (**1**), $[Tb_2L_6(H_2O)_4]\cdot 2H_2O$ (**2**) and $[Tb(phen)_2L_2(H_2O)_2](phen)L\cdot 4H_2O$ (**3**) (HL: *p*-aminobenzoic acid; phen: 1, 10-phenanthroline), with different structural forms are reported in this paper. Complex **1** is a polymolecule with a two-dimensional plane structure. Compound **2** is a binuclear molecule, and **3** appears to be a mononuclear complex. The fluorescence intensity, the fluorescence life-time and emission quantum yield of **2**, which has two coordination water molecules, is better than those of **1**, which has only one coordination water molecule. This is an unusual phenomenon for general fluorescent rare earth complexes. The fluorescence performance of **3** is the most unsatisfactory among the three complexes. Their crystal structures show that the coordination mode of the ligand is an important factor influencing the luminescence properties of a fluorescent rare earth complex.

Keywords: Rare earth; *p*-aminobenzoic acid; Crystal structure; Luminescence

1. Introduction

Fluorescent rare earth complexes are of great interest owing to their broad applications in biochemistry, material chemistry, medicine and so forth [1]. In recent years, many rare earth compounds with fluorescence have been synthesized, and the crystal structures of some complexes among them have been studied [2–17]. Zhou et al. [18] have prepared five kinds of ternary mixed ligand 4-acyl pyrazolone lanthanide complexes. Their investigation results on the fluorescence intensity and fluorescence life-time of these Tb^{3+} complexes indicate that both are dependent on the structure of the ligands; and this phenomenon has been explained by the triplet energy levels of the pyrazolone ligands. The structure of EuTETA and the luminescence properties of EuTETA and EuDOTA (TETA = 1,4,8,11-tetraazacyclo-tetradecane-1,4,8,11-tetraacetate and DOTA = 1,4,7,10-tetraazacyclododecane-1,4,7,10-tetraacetate) have been investigated by Kang et al. [19]. They have suggested that the effect of complex dehydration on their luminescence spectrum could be due to the fact that the EuTETA complex has a very labile 14-membered ring, compared to the EuDOTA complex. Martin et al. [20] have studied the effect of ligand variation on the luminescence properties of a complex, and have found substantial luminescence enhancement upon replacing terminal benzimidazole

*Corresponding authors. Fax: +86-10-6275-1708.
E-mail addresses: lijunran@pku.edu.cn (J.-R. Li), gaosong@pku.edu.cn (S. Gao).

0022-4596/$ - see front matter © 2004 Elsevier Inc. All rights reserved.
doi:10.1016/j.jssc.2004.06.038

groups with carboxamide binding units. Parker et al. [21] have set out to review lanthanide complexes which are water soluble; they highlight structural aspects of the lanthanide–water bond by a comprehensive analysis of the Cambridge Structural Database (CSD) of all published species in coordination number 9, possessing between one and nine bound water molecules, focusing on $q=1$, 2, and 9 systems; in the review, authors discussed the effect of solution pH, ligand structure, the displacement of bound water molecules and otherwise on luminescent property of lanthanide complexes, and as an example of the manner in which the Eu emission spectra signal the different structure of exchanging species, consider the competition between pH-dependent sulfonamide ligation and intramolecular carboxylate binding. These results provide good evidence that the crystal structure of a complex plays an important role in regulating its luminescence properties. However, less work has been done on the relationship between the ligand coordination mode of a complex, which would directly affect the structure of the complex, and its luminescence performance. Rare earth (RE = Nd, Dy and Yb) complexes of *p*-aminobenzoic acid have been synthesized previously [22–24]; whereas crystal structures of other rare earth complexes with this ligand have not been reported to date. In order to gain better understanding on the factors that may influence the luminescence properties of rare earth complexes, complexes **1**, **2** and **3** have been synthesized. Their crystal structures and fluorescence properties have been investigated; and the effect of ligand coordination mode on the luminescence performance of these complexes is discussed.

2. Experimental

2.1. Compound preparation

*$[Tb_2L_6(H_2O)_2]_n$ (**1**)*: This complex is obtained by the following procedure. An aqueous solution of HL (0.9 mmol), of which the pH value was adjusted to ca. 4 with aqueous ammonia, was mixed with $TbCl_3$ (0.3 mmol) under stirring. The pH value of the solution was adjusted carefully to 5.1. After filtration, the solution was left to stand at room temperature. Colorless single crystals of **1** were deposited in ca. 40% yield after one week. Anal. calcd for $TbC_{21}H_{20}N_3O_7$ (**1**): C, 43.08; N, 7.18; H, 3.42. Found: C, 42.56; N, 6.933; H, 3.370%.

*$[Tb_2L_6(H_2O)_4]\cdot 2H_2O$ (**2**)*: Colorless single crystals of **2** are obtained by following a procedure similar to the one mentioned earlier, except for the final pH value (4.0) of the solution. Complex **2** is obtained in ca. 40% yield. Anal. calcd for $TbC_{21}H_{24}N_3O_9$ (**2**): C, 40.59; N, 6.76; H, 3.89. Found: C, 40.86; N, 7.110; H, 3.513%.

*$[Tb(phen)_2L_2(H_2O)_2](phen)L\cdot 4H_2O$ (**3**)*: The preparation procedure for complex **3** is as following. First, aqueous solutions of HL (0.3 mmol) and phen (0.3 mmol) were mixed; and the pH value was adjusted to ca. 4 with aqueous ammonia. A solution of $TbCl_3$ (0.3 mmol) was then dropped into the mixed solution under stirring. Finally, the pH value of the reaction mixture was adjusted carefully to 5. After filtering, the solution was left to stand at room temperature. Colorless single crystals of complex **3** formed in ca. 45% yield after one week. Anal. calcd for $TbC_{57}H_{54}N_9O_{12}$ (**3**): C, 56.30; N, 10.37; H, 4.48. Found: C, 56.47; N, 10.10; H, 4.650%.

2.2. Instrumentation

Analyses of C, H, and N were performed on a German Elementar Vario EL instrument. IR spectra were measured using KBr pellets with a Nicolet Magna-IR 750 spectrometer at 295 K. Complexes **1**, **2** and **3** were dissolved in deionized water, respectively; and the concentrations of the solutions were all 1×10^{-3} mol/dm^3; their fluorescence spectra were then measured on a Hitachi F-4500 spectrophotometer at room temperature. The fluorescence life-times of powdered complexes **1**, **2** and **3** were determined using a Nd:YAG laser with a pulse-width of 10 ns, an excitation wavelength of 355 nm and frequency 20 Hz, and their emission quantum yields were obtained on a Hitachi F-4500 fluorescence spectrofluorometer adapted to a right-angle configuration at room temperature.

2.3. X-ray data collection and structure refinement

All data collections were carried out on a Nonius Kappa CCD diffractometer with graphite-monochromated Mo$K\alpha$ radiation (0.71073 Å) at 293 K. The structures were solved by direct methods and refined by a full-matrix least-squares technique based on F^2 using the SHELXL 97 program. All non-hydrogen atoms were refined anisotropically; and the hydrogen atoms of water molecules were located from different electronic Fourier maps. Other hydrogen atoms were placed by calculated positions and refined isotropically. Structural data, details of data collection and refinement are listed in Table 1.

3. Results and discussion

3.1. Description of the structures

*$[Tb_2L_6(H_2O)_2]_n$ (**1**)*: In this complex, each Tb^{3+} ion is chelated by one carboxyl group, coordinated by four carboxylic oxygen atoms from four ligands, one nitrogen atom from another ligand and one water molecule,

Table 1
Crystallographic data for complexes **1**, **2** and **3**

Empirical formula	$TbC_{21}H_{20}N_3O_7$ **(1)**	$TbC_{21}H_{24}N_3O_9$ **(2)**	$TbC_{57}H_{54}N_9O_{12}$ **(3)**
Crystal size (mm)	$0.20\times0.18\times0.05$	$0.3\times0.2\times0.1$	$0.2\times0.2\times0.06$
T (K)	293(2)	293(2)	293(2)
Crystal system	Monoclinic	Triclinic	Monoclinic
Space group	$P2_1/n$	$P\bar{1}$	$P2_1/c$
a (Å)	9.7278(2)	9.09640(10)	11.31300(10)
b (Å)	22.7462(4)	11.01170(10)	25.7982(3)
c (Å)	9.8147(2)	12.7430(2)	18.4017(2)
α (deg)	90.00	89.3725(5)	90.00
β (deg)	99.9410(10)	72.0360(6)	96.8156(5)
γ (deg)	90.00	75.0730(7)	90.00
V (Å^3)	2139.10(7)	1169.97(2)	5332.68(10)
Z	4	2	4
M	585.32	621.35	1216.01
D_c (g cm^{-3})	1.817	1.764	1.515
μ (mm^{-1})	3.355	3.078	1.399
F(000)	1152	616	2480
λ (Å) (Mo$K\alpha$)	0.71073	0.71073	0.71073
Monochromator	Graphite	Graphite	Graphite
θ range for data collection (deg)	3.41–27.50	3.45–27.47	3.42–27.52
Index range h; k; l	−12–12; −29–29; −12–12	−11–11; −14–14; −16–16	−14–14; −33–33; −23–23
Reflections collected	32765	24082	74052
Independent reflections	4909(R_{int} = 7.12%)	5250 (R_{int} = 4.48%)	12190 (R_{int} = 9.29%)
Observed reflections [$I>2\sigma(I)$]	2954	4813	7733
Number of parameters refined	292	350	763
R [$I>2\sigma(I)$]	0.0311	0.0313	0.0403
WR [$I>2\sigma(I)$]	0.0682	0.0772	0.0634
R (all data)	0.0655	0.0357	0.0919
WR(all data)	0.0722	0.0795	0.0720
Goodness-of-fit on F^2	0.993	1.064	1.021

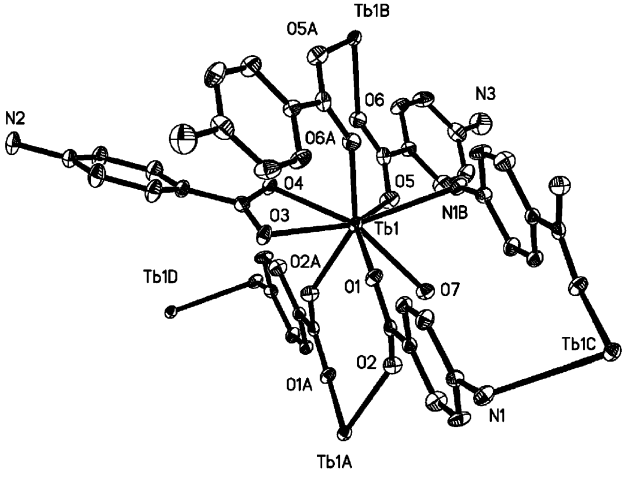

Fig. 1. An ORTEP view of complex **1** showing the connection between Tb^{3+} ions and ligands. Hydrogen atoms are omitted for clarity.

as shown in Fig. 1. The Tb^{3+} ion is, thereby, eight-coordinated by six ligands (L^-) and one H_2O molecule; and the coordination polyhedron around the Tb^{3+} ion can be described as a distorted square-antiprism. In complex **1**, the ligands coordinated to the Tb^{3+} ion have three different coordination modes (modes 1, 2 and 3). In coordination mode 1, L^- acts as a tridentate ligand coordinating to three Tb^{3+} ions (Tb1, Tb1A and Tb1C); that is, its carboxyl group connects two neighboring Tb^{3+} ions (Tb1 and Tb1A), and its amino group coordinates to a third Tb^{3+} ion (Tb1C). In mode 2, the carboxyl group of the ligand acts as a bidentate bridge connecting two Tb^{3+} ions (Tb1 and Tb1B). Therefore, the Tb^{3+} ions are bridged through the carboxyl groups in both modes 1 and 2 to form a one-dimensional chain. In addition, the amino groups of mode 1 ligands in a chain are coordinated to Tb^{3+} ions from two adjacent chains, resulting in a two-dimensional plane (Fig. 2). In mode 3, the carboxyl groups chelate the Tb^{3+} ions. In both modes 2 and 3, the amino groups are not involved in coordination with the Tb^{3+} ions.

In complex **1**, the uncoordinated amino groups of the ligands in mode 3, and the coordination water (O7–H2w$\cdots$N2[$-x+3/2$, $y-1/2$, $-z+1/2$] = 2.910 Å) or the carboxyl groups (N2–H2b$\cdots$O3[$x+1/2$, $-y+1/2$, $z+1/2$] = 2.973 Å) from adjacent layers, are linked together through hydrogen bonds, forming a three-dimensional structure. The hydrogen bonds between the coordination water molecules and the coordinated or uncoordinated amino groups, and the hydrogen bonds between the coordinated amino groups and the carboxyl groups, respectively, are in a plane [see Table 2 (a)]. In a coordination unit, a hydrogen bond is also found

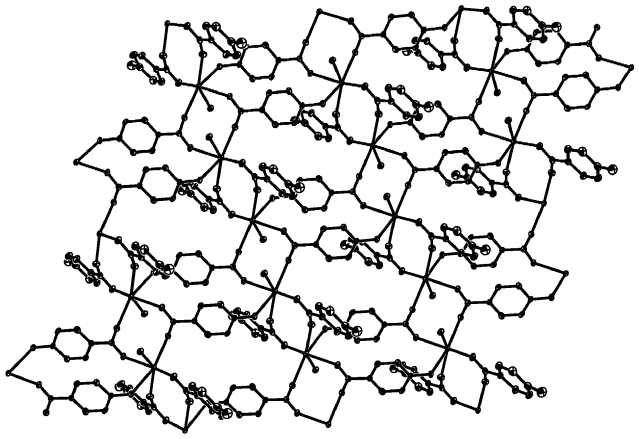

Fig. 2. A two-dimensional structure of complex **1** showing the connection between the chains. Hydrogen atoms and the L^- ligands in mode 3 are omitted for clarity.

between the coordination water and the carboxyl group (O7–H1w···O2 = 2.774 Å) [see Table 2 (a)]. Selected bond lengths and angles, including hydrogen bonds, are listed in Table 2 (a).

Complex **2** is a binuclear molecule with two carboxyl groups acting as bidentate bridges between the two Tb^{3+} ions. Each Tb^{3+} ion is, in addition, chelated by two carboxyl groups and coordinated by two H_2O molecules. The amino groups in the ligands are not coordinated to the Tb^{3+} ions (Fig. 3). Consequently, the eight oxygen atoms surrounding the Tb^{3+} ion form a distorted square-antiprism coordination polyhedron. Moreover, in the crystal structure of complex **2**, the coordination H_2O molecules in one binuclear molecule are linked to amino groups (O8–H3w···N2[$x+1$, $y-1$, z] = 2.741 Å) or the carboxyl group (O7–H1w···O1 [$-x+2$, $-y+2$, $-z+1$] = 2.786 Å) from adjacent binuclear molecules through hydrogen bonds. Uncoordinated H_2O molecules are also linked to ligand amino groups or carboxyl groups through hydrogen-bonding [see Table 2 (b)]. Selected bond lengths and angles, including hydrogen bonds, are listed in Table 2 (b).

In the mononuclear complex **3**, the Tb^{3+} ion is chelated by two phen molecules, and coordinated by two oxygen atoms from two L^- ligands in monodentate coordination mode; in addition, two H_2O molecules also participate in coordination (Fig. 4). The eight atoms coordinated to the Tb^{3+} ion thereby form a distorted square-antiprism. In the crystal structure, uncoordinated phen molecules are linked to the coordination units through hydrogen bonds (O6–H3w···N8[x, $-y+3/2$, $z+1/2$] = 2.876 Å) between nitrogen atoms and coordination H_2O molecules. Uncoordinated L^- ions and the coordination units are also joined by hydrogen bonds (O5–H2w···O8 = 2.613 Å; N6–H6b···O8[$-x$, $-y+1$, $-z+1$] = 2.934 Å) between carboxyl groups and coordination water molecules or amino groups from the L^- ligands [see Table 2 (c)]. In addition, crystalline water molecules and carboxyl groups or amino groups of the L^- ligands, crystalline water molecules and carboxyl groups or amino groups of the L^- ions, crystalline water molecules and coordination water molecules or neighboring crystalline water molecules, are all interconnected by hydrogen bonds, respectively, in the crystal [see Table 2 (c)]. Selected bond lengths and angles, including hydrogen bonds, are listed in Table 2 (c).

3.2. IR characterization

The infrared spectra of complexes **1**–**3** have in common the occurrence of a strong and broad absorption centered at ca. 3400 cm^{-1}, which can be attributed to the OH stretching of both coordinated and crystalline water molecules. The IR absorptions of the carboxylate moiety, ν_{as}(OCO) and ν_s(OCO), in free L^- ion and coordinated L^- ligands are compared. After coordination to the Tb^{3+} ion, the ν_{as}(OCO) absorption is found to have red-shifted 12 cm^{-1}, from 1601 to 1589 cm^{-1}; the ν_s(OCO) absorption at 1423 cm^{-1} has shifted from 25 cm^{-1} down to 1398 cm^{-1}, for complex **1**. For complex **2**, the IR absoptions (ν_{as}(OCO) = 1592 cm^{-1}, ν_s(OCO) = 1417 cm^{-1}) of the carboxyl group are similar to that of complex **1**. However, the value of ν_s(C–N) is obviously different for complex **1** and complex **2**: the ν_s(C–N) absorption in complex **1** has red-shifted 30 cm^{-1}, from 1326 to 1296 cm^{-1}; whereas the ν_s(C–N) absorption shift in complex **2** (1324 cm^{-1}) is negligible, comparing to that in free L^- ions. The above observations indicate that the carboxyl groups of the L^- ligands are coordinated to the Tb^{3+} ions, and the coordination modes in complex **1** and **2** are similar. There are L^- ligands whose amino groups are coordinated to Tb^{3+} ions in complex **1**; however, no such L^- ligands exist in complex **2** [25]. The infrared spectra of complex **3** show absorptions of ν_{as}(OCO), ν_s(OCO) and ν_s(C–N) at 1600, 1396, 1611, 1375 and 1327 cm^{-1}, suggesting that two types of carboxyl groups, coordinated and free, exist in the structure of complex **3**; and the amino groups do not participate in the coordination with Tb^{3+} ions [25], which is consistent with the structural analysis results.

3.3. Luminescence property of the complexes

The emission spectra (see Fig. 5) at excitation wavelengths (λ_{ex}) 320, 319 and 320 nm, the fluorescence life-time of $^5D_4$ energy and emission quantum yield, for complexes **1**, **2** and **3**, are obtained, respectively. There are four spectral bands at emission wavelengths (λ_{em}) ca. 491, 545, 585 and 621 nm in the emission spectra, which correspond to the $^5D_4 \rightarrow {}^7F_6$, $^5D_4 \rightarrow {}^7F_5$, $^5D_4 \rightarrow {}^7F_4$ and $^5D_4 \rightarrow {}^7F_3$ electronic transitions, respectively, in the Tb^{3+} ion. In order to compare the fluorescence property

Table 2
Selected bond lengths (Å) and angles (°)

a Complex **1**

Bond lengths (Å)				
Tb(1)–O(6)#1	2.287(3)	Tb(1)–O(4)	2.446(3)	
Tb(1)–O(5)	2.319(3)	Tb(1)–O(3)	2.452(3)	
Tb(1)–O(1)	2.327(2)	Tb(1)–O(7)	2.499(3)	
Tb(1)–O(2)#2	2.335(3)	Tb(1)–N(1)#3	2.688(3)	
Bond angles (deg)				
O(6)#1–Tb(1)–O(5)	103.29(10)	O(6)#1–Tb(1)–O(1)	92.77(10)	
O(5)–Tb(1)–O(1)	143.97(10)	O(6)#1–Tb(1)–O(2)#2	148.42(10)	
O(5)–Tb(1)–O(2)#2	89.09(10)	O(1)–Tb(1)–O(2)#2	93.78(10)	
O(6)#1–Tb(1)–O(4)	77.07(10)	O(5)–Tb(1)–O(4)	87.57(10)	
O(1)–Tb(1)–O(4)	127.78(9)	O(2)#2–Tb(1)–O(4)	74.53(9)	
O(6)#1–Tb(1)–O(3)	79.65(10)	O(5)–Tb(1)–O(3)	139.71(9)	
O(1)–Tb(1)–O(3)	74.41(9)	O(2)#2–Tb(1)–O(3)	72.49(10)	
O(4)–Tb(1)–O(3)	53.42(8)	O(6)#1–Tb(1)–O(7)	138.09(10)	
O(5)–Tb(1)–O(7)	71.10(10)	O(1)–Tb(1)–O(7)	75.39(9)	
O(2)#2–Tb(1)–O(7)	73.33(10)	O(4)–Tb(1)–O(7)	141.35(10)	
O(3)–Tb(1)–O(7)	132.06(9)	O(6)#1–Tb(1)–N(1)#3	69.29(10)	
O(5)–Tb(1)–N(1)#3	74.71(10)	O(1)–Tb(1)–N(1)#3	81.44(9)	
O(2)#2–Tb(1)–N(1)#3	142.28(10)	O(4)–Tb(1)–N(1)#3	136.57(9)	
O(3)–Tb(1)–N(1)#3	139.38(10)	O(7)–Tb(1)–N(1)#3	69.24(10)	
Hydrogen bonds				
D–H···A	*D*–H/Å	H···A/Å	*D*–H···A/°	*D*···A/Å
N1–H1a···O7[$-x,-y,-z$]	0.860	2.225	142.13	2.951
N1–H1b···O6[$x-1,y,z-1$]	0.860	2.355	116.76	2.847
N2–H2a	0.860			
N2–H2b···O3[$x+1/2,-y+1/2,z+1/2$]	0.860	2.291	136.29	2.973
N3–H3a···O7[$x+1/2,-y-1/2,z+1/2$]	0.860	2.305	157.06	3.115
N3–H3b	0.860			
O7–H2w···N2[$-x+3/2,y-1/2,-z+1/2$]	0.910	2.054	156.35	2.910
O7–H1w···O2	0.934	1.947	146.47	2.774

A = acceptor, D = donor, w = water
Symmetry transformations used to generate equivalent atoms: #1$-x+1,-y,-z+1$; #2$-x+1,-y,-z$; #3$-x,-y,-z$.

b Complex **2**

Bond lengths (Å)				
Tb(1)–O(3)	2.277(2)	Tb(1)–O(4)#1	2.264(3)	
Tb(1)–O(8)	2.351(2)	Tb(1)–O(6)	2.367(2)	
Tb(1)–O(7)	2.419(2)	Tb(1)–O(2)	2.422(2)	
Tb(1)–O(5)	2.504(2)	Tb(1)–O(1)	2.514(2)	
Bond angles (deg)				
O(4)#1–Tb(1)–O(3)	109.24(12)	O(4)#1–Tb(1)–O(8)	86.79 (12)	
O(3)–Tb(1)–O(8)	156.27(10)	O(4)#1–Tb(1)–O(6)	83.83(11)	
O(3)–Tb(1)–O(6)	123.23(10)	O(8)–Tb(1)–O(6)	74.57(9)	
O(4)#1–Tb(1)–O(7)	73.33(10)	O(3)–Tb(1)–O(7)	80.86(10)	
O(8)–Tb(1)–O(7)	87.51(9)	O(6)–Tb(1)–O(7)	151.74(10)	
O(4)#1–Tb(1)–O(2)	163.25(11)	O(3)–Tb(1)–O(2)	77.24(11)	
O(8)–Tb(1)–O(2)	92.36(11)	O(6)–Tb(1)–O(2)	79.83(9)	
O(7)–Tb(1)–O(2)	123.37(8)	O(4)#1–Tb(1)–O(5)	74.96(10)	
O(3)–Tb(1)–O(5)	76.34(9)	O(8)–Tb(1)–O(5)	125.92(8)	
O(6)–Tb(1)–O(5)	53.45(8)	O(7)–Tb(1)–O(5)	131.69(8)	
O(2)–Tb(1)–O(5)	92.21(8)	O(4)#1–Tb(1)–O(1)	142.93(10)	
O(3)–Tb(1)–O(1)	78.24(9)	O(8)–Tb(1)–O(1)	78.53(9)	
O(6)–Tb(1)–O(1)	123.45(8)	O(7)–Tb(1)–O(1)	72.20(8)	
O(2)–Tb(1)–O(1)	52.54(8)	O(5)–Tb(1)–O(1)	140.37(8)	
Hydrogen bonds				
D–H···A	*D*–H/Å	H···A/Å	*D*–H···A/°	*D*···A/Å
N1–H1a	0.810			
N1–H1b···O9[$x+1,y+1,z$]	0.854	2.262	151.20	3.038
O7–H1w···O1[$-x+2,-y+2,-z+1$]	0.935	1.856	173.08	2.786
N2–H2a···O1[$-x+1,-y+3,-z+1$]	0.728	2.659	164.26	3.365

Table 2 (*continued*)

b Complex **2**

N2–H2b	0.756			
O7–H2w···O5[$-x+1,-y+2,-z+1$]	0.918	1.865	167.32	2.768
N3–H3a	0.699			
N3–H3b···O9	0.874	2.093	155.70	2.912
O8–H3w···N2[$x+1,y-1,z$]	0.938	1.803	178.85	2.741
O8–H4w···N1[$x,y-1,z$]	0.955	1.998	158.78	2.909
O9–H5w···O6[$x-1,y,z$]	0.960	1.996	149.12	2.863
O9–H6w···O2[$-x,-y+2,-z+2$]	0.953	1.914	154.30	2.803

A = acceptor, D = donor, w = water

Symmetry transformations used to generate equivalent atoms: #1 $-x+1,-y+2,-z+1$.

c Complex **3**

Bond lengths (Å)			
Tb(1)–O(3)	2.2851(19)	Tb(1)–O(1)	2.3122(19)
Tb(1)–O(5)	2.314(2)	Tb(1)–O(6)	2.417(2)
Tb(1)–N(2)	2.533(3)	Tb(1)–N(4)	2.554(3)
Tb(1)–N(3)	2.554(3)	Tb(1)–N(1)	2.558(3)
Bond angles (deg)			
O(3)–Tb(1)–O(1)	143.89(7)	O(3)–Tb(1)–O(5)	83.62(8)
O(1)–Tb(1)–O(5)	75.02(8)	O(3)–Tb(1)–O(6)	76.96(8)
O(1)–Tb(1)–O(6)	133.80(8)	O(5)–Tb(1)–O(6)	147.57(8)
O(3)–Tb(1)–N(2)	140.87(8)	O(1)–Tb(1)–N(2)	73.43(8)
O(5)–Tb(1)–N(2)	103.23(8)	O(6)–Tb(1)–N(2)	77.62(8)
O(3)–Tb(1)–N(4)	109.50(8)	O(1)–Tb(1)–N(4)	71.42(7)
O(5)–Tb(1)–N(4)	137.59(8)	O(6)–Tb(1)–N(4)	74.14(8)
N(2)–Tb(1)–N(4)	91.37(9)	O(3)–Tb(1)–N(3)	74.27(8)
O(1)–Tb(1)–N(3)	74.25(8)	O(5)–Tb(1)–N(3)	82.22(8)
O(6)–Tb(1)–N(3)	116.24(8)	N(2)–Tb(1)–N(3)	144.44(8)
N(4)–Tb(1)–N(3)	64.36(9)	O(3)–Tb(1)–N(1)	80.32(8)
O(1)–Tb(1)–N(1)	121.07(8)	O(5)–Tb(1)–N(1)	76.53(8)
O(6)–Tb(1)–N(1)	74.79(8)	N(2)–Tb(1)–N(1)	64.55(9)
N(4)–Tb(1)–N(1)	144.05(8)	N(3)–Tb(1)–N(1)	148.41(9)

Hydrogen bonds

D–H···A	*D*–H/Å	H···A/Å	*D*–H···A/°	*D*···A/Å
N5–H5a···	0.860			
N5–H5b···O10[$x-1,y,z$]	0.860	2.282	152.70	3.071
N6–H6a···O12[$-x+1,-y+1,-z+1$]	0.860	2.327	140.59	3.040
N6–H6b···O8[$-x,-y+1,-z+1$]	0.860	2.139	153.47	2.934
O5–H2w···O8	0.911	1.709	171.39	2.613
O5–H1w···O2	0.908	1.795	162.46	2.675
O10–H8w···O9	0.934	1.935	148.37	2.773
O12–H12w···O2[$x+1,y,z$]	0.924	1.871	168.98	2.784
O6–H3w···N8[$x,-y+3/2,z+1/2$]	0.928	2.101	140.18	2.876
O12–H11w···O4	0.947	1.833	167.68	2.765
O9–H6w···O12[$x,-y+3/2,z-1/2$]	0.938	1.981	175.83	2.917
O9–H5w···O7[$x+1,-y+3/2,z-1/2$]	0.912	1.941	162.52	2.824
O11–H10w···O7	0.919	2.014	162.26	2.903
O6–H4w···O4	0.924	1.788	173.43	2.708
O11–H9w···O10[$x-1,-y+3/2,z+1/2$]	0.926	1.976	166.35	2.884
O10–H7w···N9[$x,-y+3/2,z-1/2$]	0.905	2.263	160.76	3.132

A = acceptor, D = donor, w = water

of the three complexes, the relative intensity of the spectral band at ca. 545 nm, which is the most intensive of all four bands, has been chosen as a representative. The results show that the relative fluorescence intensity (71.25) of complex **2** is stronger than that (27.44) of complex **1**, and complex **2** displays longer fluorescence life-time (580 μs) and better emission quantum yield (0.67) than complex **1** (490 μs and 0.53), although complex **2** has two coordination water molecules per Tb^{3+} ion and complex **1** has only one coordination water molecule per Tb^{3+} ion. The compositions of complexes **1** and **2** are the same except for the number of H_2O molecules. As common knowledge [1], the coordination of water molecule would decrease the

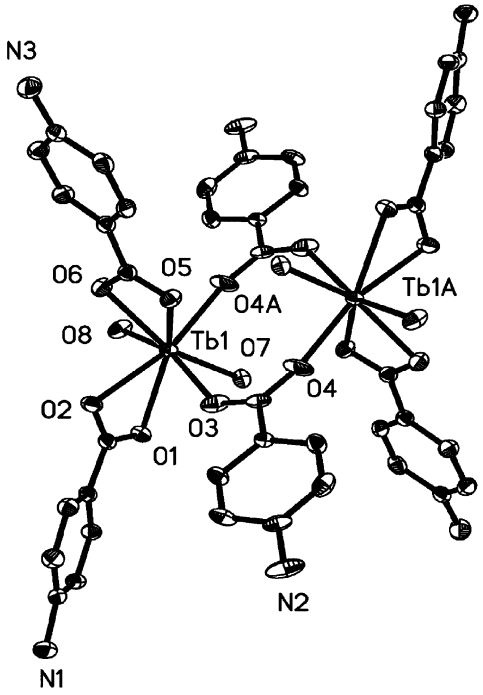

Fig. 3. An ORTEP view of complex **2** showing the connection between Tb^{3+} ions and ligands. Hydrogen atoms and crystal water molecule are omitted for clarity.

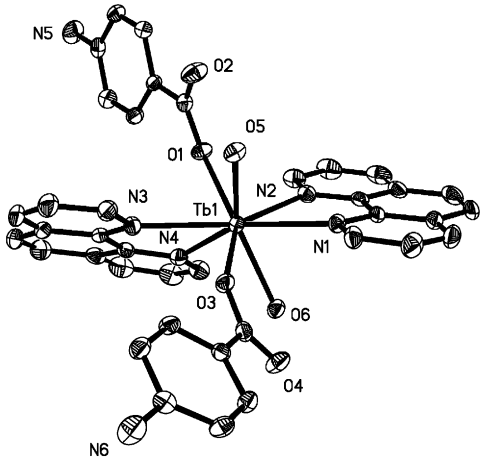

Fig. 4. An ORTEP view of complex **3** showing the connection between Tb^{3+} ions and ligands. Hydrogen atoms, crystal water molecules, uncoordinated phen and L^- ion are omitted for clarity.

fluorescence intensity of a rare earth complex because the thermal vibration of water molecules would consume part of the energy absorbed by the ligand. The unusual result obtained in our experiments indicates that the structure of a complex could be the dominant factor that influences its fluorescence property. The crystal structure of complex **2** is distinct from that of complex **1**. The above observations show that the ligand coordination mode in complex **2** makes the energy transfer from the ligand L^- to the Tb^{3+} ion more effective than that in complex **1**. That is, the lowest

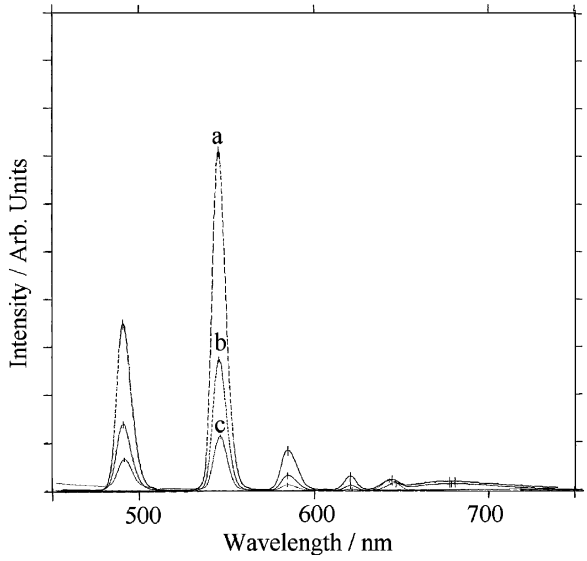

Fig. 5. The emission spectra of complexes **1(b)**, **2(a)** and **3(c)**.

triplet state energy level of ligand L^- and the lowest exited state energy level of the Tb^{3+} ion is better matched in the structure of complex **2** than in that of complex **1**. The relative fluorescence intensity (11.36) of complex **3**, which has two coordination phen molecules per Tb^{3+} ion, is the weakest, and its fluorescence lifetime (250 μs) and the emission quantum yield (0.19) are the lowest, respectively, among all three terbium complexes. This phenomenon has been explained previously in literature [26]. Xi-Juan Yu and Qing-De Su studied the photoacoustic (PA) amplitude spectra and luminescence spectra of the $Tb(Benz)_3$, $Tb(Benz)_3(phen)$ and $Tb(Benz)_3(bpy)$ complexes (Benz: benzoic acid; bpy: 2,2′-bipyridine) [26]. In contrast to the effect of using bpy as the second ligand, the luminescence intensity and the PA phase data decreased greatly when phen was introduced instead as the second ligand into the $Tb(Benz)_3$ complex. The authors suggested that an energy gap exists between the ligand triplet state and the resonance level of the rare earth ion. Part of the energy absorbed by Benz may be transferred to the second ligand (e.g., phen) first, before being transferred to the Tb^{3+} ion. However, the energy gap is so small that the inverse energy transfer rate from the thermally activated Tb^{3+} ion to the second ligand (phen) increases more, making the luminescence intensity of the $Tb(Benz)_3(phen)$ complex the lowest of all three complexes. The energy transfer process in complex **3** may be similar to that in the $Tb(Benz)_3(phen)$ complex, which renders the fluorescence intensity of complex **3** the lowest of complexes **1**, **2** and **3**.

As discussed earlier, the ligand coordination mode in a complex may be a crucial factor that influences the match between the lowest triplet state energy level of the ligand and the lowest exited state energy level of the

Tb^{3+} ion; which, in turn, influences the luminescence property of the complex. To compare the coordination modes of L^- ligands in complexes **1**, **2** and **3**, the average number ($1+2\times1/2+3\times1/3=3$) of L^- ligands coordinated to a Tb^{3+} ion in complex **1** is found equal to that ($2+2\times1/2=3$) in complex **2**; however, the number (2) of L^- ligands, which coordinate with bidentate chelating carboxyl groups, is larger in complex **2** than that (1) in complex **1**. In addition, three of the six L^- ligands surounding a Tb^{3+} ion are shared by three Tb^{3+} ions in complex **1**; in complex **3**, however, each Tb^{3+} ion is only coordinated by two L^- ligands with monodentate carboxyl groups. This may be due to steric hinderance caused by phen coordination. These structural differences suggest that both the average number of ligands and ligand coordination mode around a Tb^{3+} ion can influence the luminescence property of the complex; however, between these two factors, the effect of coordination mode should be more pronounced when the average number of ligands is the same. The energy transfer from the L^- ligand to the Tb^{3+} ion may be more effective for the coordination modes using bidentate chelating carboxyl groups than for other coordination modes. Energy transfer may be more favorable when a L^- ligand is not coordinated to more than one Tb^{3+} ions. Alternately, mode 3 may be the most effective ligand coordination mode for energy transfer, and the efficiency of energy transfer may be reduced when an L^- ligand, such as the L^- ligands in modes 1 and 2, is coordinated to more than one Tb^{3+} ions. Therefore, even though containing more H_2O molecules than complexes **1** and **3**, complex **2** still has the strongest fluorescence of all three because each Tb^{3+} ion is chelated by more L^- ligands in mode 3. The fluorescence intensity of complex **3** is weaker than that of complex **1**, this may be explained by the facts that complex **3** has no chelating carboxyl groups and it also has less L^- ligands coordinated to Tb^{3+} ions than complex **1**.

4. Conclusions

Three new terbium complexes have been prepared and structurally characterized. Their luminescence properties have been studied, and the results show that the coordination mode of the ligand can be a important factor that influences the energy transfer between the ligand and the center ion; which, in turn, influences the fluorescence intensity of a complex. Energy transfer from the L^- ligand to the Tb^{3+} ion may be more effective for coordination modes using bidentate chelating carboxyl groups than other coordination modes. Energy transfer may be more favorable when an L^- ligand is not coordinated to more than one Tb^{3+} ions. The efficiency of energy transfer may be reduced when an L^- ligand is coordinated to more Tb^{3+} ions.

Acknowledgments

The authors would like to acknowledge support from the National Science Foundation for Distinguished Young Scholars (20125104, 20221101), the National Key Project for Fundamental Research (G1998061305) and NHTRDP (863 Program) of P.R. China (2002AA324080).

References

[1] C.H. Huang, Rare Earth Coordination Chemistry, Science Press, Mascow, 1997, pp. 363–388 (in Chinese).
[2] B.L. An, M.L. Gong, J.M. Zhang, S.L. Zheng, Polyhedron 22 (19) (2003) 2719–2724.
[3] Y.H. Hou, C.X. Du, Y. Zhu, Z.X. Zhou, Acta Chim. Sinica 61 (3) (2003) 367–371.
[4] G. Oczko, J. Legendziewicz, V. Trush, V. Amirkhanov, New J. Chem. 27 (6) (2003) 948–956.
[5] J.B. Yu, H.J. Zhang, L.S. Fu, R.P. Deng, L. Zhou, H.R. Li, F.Y. Liu, H.L. Fu, Inorg. Chem. Commun. 6 (7) (2003) 852–854.
[6] H. Deng, Y.P. Cai, H. Chao, C.L. Chen, C.W. Jiang, C.Q. Chen, L.N. Ji, Chinese J. Chem. 21 (4) (2003) 409–414.
[7] X.J. Zheng, L.P. Jin, Z.M. Wang, C.H. Yan, S.Z. Lu, Q. Li, Polyhedron 22 (2) (2003) 323–330.
[8] H.B. Liu, B.L. Li, H.Q. Wang, Z. Xu, Chinese J. Chem. 19 (8) (2001) 766–771.
[9] C. Tedeschi, C. Picard, J. Azema, B. Donnadieu, P. Tisnes, New J. Chem. 24 (10) (2000) 735–737.
[10] J.G. Mao, T.C.W. Mak, H.J. Zhang, J.Z. Ni, S.B. Wang, J. Coordination Chem. 47 (1) (1999) 145–154.
[11] J.G. Mao, H.J. Zhang, J.Z. Ni, S.B. Wang, T.C.W. Mak, Polyhedron 17 (23–24) (1998) 3999–4009.
[12] L.G. Zhu, H.P. Xiao, J. Rare Earths 20 (5) (2002) 400–403.
[13] R.G. Xiong, J.L. Zuo, Z. Yu, X.Z. You, W. Chen, Inorg. Chem. Commun. 2 (10) (1999) 490–494.
[14] G. Vicentini, K. Zinner, Polyhedron 14 (20–21) (1995) 3067–3076.
[15] Z.M. Zheng, L.P. Jin, M.Z. Wang, J.H. Zhang, S.Z. Lu, Chem. J. Chinese Universities-Chinese 16 (7) (1995) 1007–1011.
[16] P.R. Selvin, J. Jancarik, M. Li, L.W. Hung, Inorg. Chem. 35 (3) (1996) 700–705.
[17] H.Y. Sun, C.H. Huang, X.L. Jin, G.X. Xu, Polyhedron 14 (9) (1995) 1201–1206.
[18] D.J. Zhou, Q. Li, C.H. Huang, G.Q. Yao, S.G. Umetani, M.K. Matsui, L.M. Ying, A.C. Yu, X.S. Zhao, Polyhedron 16 (8) (1997) 1381–1389.
[19] J.G. Kang, M.K. Na, S.K. Yoon, Y. Sohn, Y.D. Kim, I.H. Suh, Inorg. Chim. Acta 310 (1) (2000) 56–64.
[20] N. Martin, J.C.G. Bunzli, V. McKee, C. Piguet, G. Hopfgartner, Inorg. Chem. 37 (3) (1998) 577–589.
[21] D. Parker, R.S. Dickins, H. Puschmann, C. Crossland, J.A.K. Howard, Chem. Rev. 102 (2002) 1977–2010.
[22] Z. Rzaczyńska, V.K. belsky, Polish J. Chem. 68 (1994) 309–319.
[23] M.S. Khiyalov, I.R. Amirasłanov, Kh.S. Mamedov, E.M. Movsumov, Zh. Strukt. Khim. 22 (3) (1981) 113–119.
[24] M.S. Khiyalov, I.R. Amirasłanov, Kh.S. Mamedov, E.M. Movsumov, Koord. Khim. 7 (3) (1981) 445–449.
[25] K. Nakamoto, Infrared Spectra of Inorganic and Coordination Compound, fourth Edition, Wiley, New York, 1986, pp. 258.
[26] X.J. Yu, Q.D. Su, J. Photochem. Photobiol. A: Chemistry 155 (2003) 73–78.